

A Higgs Conundrum with Vector Fermions

S. Dawson and E. Furlan

Department of Physics, Brookhaven National Laboratory, Upton, NY 11973, USA

Abstract

Many models of Beyond the Standard Model physics involve heavy colored fermions. We study models where the new fermions have vector interactions and examine the connection between electroweak precision measurements and Higgs production. In particular, for parameters which are allowed by precision measurements, we show that the gluon fusion Higgs cross section and the Higgs decay branching ratios must be close to those predicted by the Standard Model. The models we discuss thus represent scenarios with new physics which will be extremely difficult to distinguish from the minimal Standard Model. We pay particular attention to the decoupling properties of the vector fermions.

I. INTRODUCTION

The Standard Model of particle physics has a remarkable body of experimental support, but the Higgs boson remains a missing ingredient. Precision electroweak measurements suggest that a Standard Model Higgs boson must be lighter than ~ 145 GeV [1, 2] and recent measurements from the LHC exclude a Standard Model Higgs boson in the range $129 \text{ GeV} < M_H < 600 \text{ GeV}$ [3]. Preliminary measurements suggest a light Higgs boson in the mass region $M_H \sim 125 \text{ GeV}$ [3, 4]. Should this putative Higgs signal be confirmed, the pressing issue will be understanding its properties.

For all Higgs masses, gluon fusion is the dominant production mechanism at hadron colliders and the production rate is well understood up to NNLO in QCD [5, 6]. Theoretical uncertainties from renormalization/factorization scale choices and from the choice of parton distribution functions are also well understood [7–10]. The total rate, however, is sensitive to the existence of colored particles which couple to the Higgs boson. Beyond the Standard Model physics can potentially have a large effect on the Higgs boson production rate, making this a window to high scale physics [8, 11–13].

The effects on Higgs production of squarks, Kaluza Klein colored fermions, color octet scalars, fermionic top quark partners and 4th generation fermions (among many others) have been extensively studied. The simplest possibility for new heavy fermions is to form a chiral heavy new generation which, except for masses, is an exact copy of the known generations. After careful tuning, it is possible to find combinations of 4th generation fermion masses which are permitted by precision electroweak measurements [14, 15] and are not excluded by direct searches. Since a chiral 4th generation quark is assumed to couple to the Higgs boson with a strength proportional to its mass, heavy quarks do not decouple from the production of the Higgs boson (and in fact increase the rate by a factor of ~ 9). the existence of a 4th generation of fermions would exclude a Higgs boson mass up to $M_H \sim 600 \text{ GeV}$ [16] regardless of the fermion masses.

In this paper, we study the effect of heavy vector quarks on Higgs boson production and study both the case of an isospin singlet top partner and an isospin doublet of heavy fermions. A vector singlet top partner arises naturally in Little Higgs models [17–23], where the couplings to the Higgs boson of the top quark and its fermion partner are fixed in such a manner as to cancel their quadratically divergent contributions to the Higgs mass

renormalization. Top-quark fermion partners are also found in top color [24, 25] and top condensate [26–29] models where there is a natural hierarchy of scales such that the top partner obtains a large Dirac mass. Light vector fermions instead typically appear in composite Higgs models [30–33]. Our results are general enough to be applied to any of these models and hence represent a simplification of results which have previously been presented in the context of very specific scenarios.

A study of the S , T , U parameters and the $Z \rightarrow b\bar{b}$ decay rate [34, 35] restricts the allowed parameter space for heavy vector fermions. However, vector fermions have interesting decoupling properties as the mixing with the Standard Model fermions becomes small, which makes a large region of parameter space experimentally viable. Vector fermions which couple to the Standard Model fermions and Higgs boson can be $SU(2)_L$ singlets with the same hypercharge as the Standard Model right-handed quarks, doublets with $Y = Y_{SM} = \frac{1}{6}$ or $Y = Y_{SM} \pm 1$, or triplets with $Y = Y_{SM} \pm \frac{1}{2}$ [36]. We consider the “Standard Model-like” case with either a heavy fermion singlet of charge 2/3 or a doublet with the Standard Model assignments of hypercharge. We compute the NNLO prediction for Higgs production for the allowed parameter region of these models and quantify the allowed deviation from the Standard Model prediction. The new features of our study include up-to-date fits to precision electroweak measurements in models with vector fermions, and an analysis of the the resulting consequences for Higgs boson production at NNLO in perturbative QCD.

II. THE MODELS

We consider models with additional vector-like charge 2/3 quarks, \mathcal{T}^α , and charge -1/3 quarks, \mathcal{B}^α , which mix with the Standard Model-like third generation quarks. For simplicity we make the following assumptions:

- the electroweak gauge group is the standard $SU(2)_L \times U(1)_Y$ group;
- there is only a single Standard Model Higgs $SU(2)_L$ doublet,

$$H = \begin{pmatrix} \phi^+ \\ \phi^0 \end{pmatrix}, \quad (1)$$

with $\phi^0 = \frac{v+h}{\sqrt{2}}$;

- we neglect generalized CKM mixing and only allow mixing between the Standard Model-like third generation quarks and at most one new charge 2/3 quark singlet or one new $SU(2)_L$ quark doublet. We do not consider fermions in more exotic representations.

The Standard Model-like chiral fermions are

$$\psi_L^1 = \begin{pmatrix} \mathcal{T}_L^1 \\ \mathcal{B}_L^1 \end{pmatrix}, \quad \mathcal{T}_R^1, \mathcal{B}_R^1, \quad (2)$$

with the Lagrangian describing the fermion masses

$$-\mathcal{L}_M^{SM} = \lambda_1 \bar{\psi}_L^1 H \mathcal{B}_R^1 + \lambda_2 \bar{\psi}_L^1 \tilde{H} \mathcal{T}_R^1 + \text{h.c.}, \quad (3)$$

and $\tilde{H} = i\sigma_2 H^*$.

The models we consider are:

- singlet fermion model: add a vector $SU(2)_L$ quark singlet of charge 2/3, \mathcal{T}_L^2 and \mathcal{T}_R^2 .
- doublet fermion model: add a vector $SU(2)_L$ doublet of hypercharge 1/6,

$$\psi_L^2 = \begin{pmatrix} \mathcal{T}_L^2 \\ \mathcal{B}_L^2 \end{pmatrix}, \quad \psi_R^2 = \begin{pmatrix} \mathcal{T}_R^2 \\ \mathcal{B}_R^2 \end{pmatrix}. \quad (4)$$

III. EXPERIMENTAL LIMITS ON TOP PARTNER MODELS

A. Limits from R_b and A_b

Data from LEP and SLD place stringent restrictions on the couplings of the fermionic top partners. The top partners mix with the Standard Model-like top quark and contribute at one loop to processes involving bottom quarks, especially $Z \rightarrow b\bar{b}$ and A_b . The neutral current couplings to the bottom can be parametrized by the effective Lagrangian

$$\mathcal{L}^{NC} = \frac{g}{c_W} Z_\mu \bar{f} \gamma^\mu \left[\left(g_L^f + \delta \tilde{g}_L^f \right) \left(\frac{1 - \gamma_5}{2} \right) + \left(g_R^f + \delta \tilde{g}_R^f \right) \left(\frac{1 + \gamma_5}{2} \right) \right] f, \quad (5)$$

where the Standard Model couplings are normalized such that $g_L^f = T_3^f - Q_f s_W^2$, $g_R^f = -Q_f s_W^2$, with $s_W^2 \equiv \sin^2 \theta_W = (e/g)^2 = 0.231$ [37] and $T_3^f = \pm 1/2$. The couplings $\delta \tilde{g}_{L,R}^f \equiv \delta g_{L,R}^{f,SM} + \delta g_{L,R}^f$ contain both the Standard Model radiative corrections, $\delta g_{L,R}^{f,SM}$, and

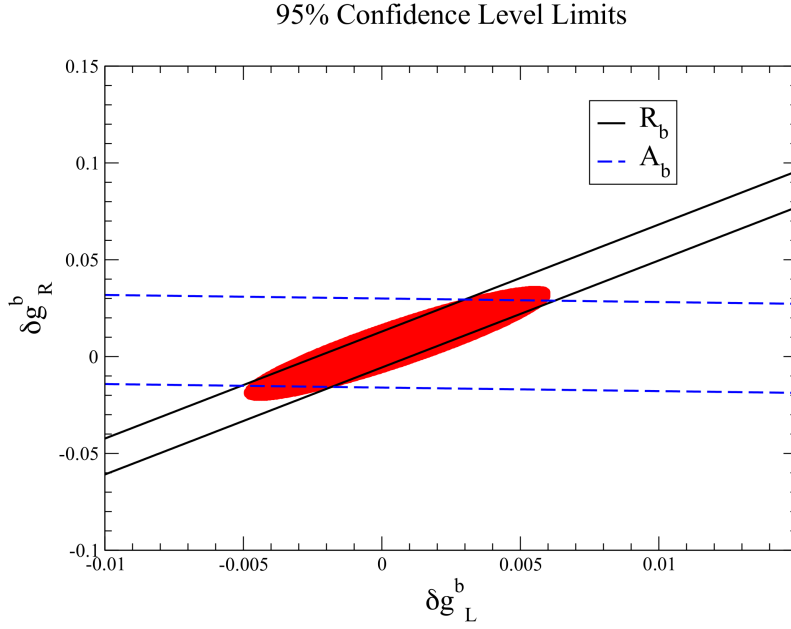


FIG. 1: Allowed 95% confidence level regions from the simultaneous fit to R_b and A_b (red shaded), R_b alone (between solid black lines), and A_b alone (between dashed blue lines).

the new physics contributions, $\delta g_{L,R}^f$. The Standard Model contribution from top quark loops is well known [38–40], and in the limit $m_t \gg M_Z$ it is given by

$$\delta g_L^{b,SM} = \frac{G_F m_t^2}{\sqrt{2} 8\pi^2}. \quad (6)$$

The dominant effect of new physics in the b sector can be found by assuming that δg_L^b and δg_R^b are small and approximating [41, 42]

$$\begin{aligned} R_b &= \frac{\Gamma(Z \rightarrow b\bar{b})}{\Gamma(Z \rightarrow \text{hadrons})} = R_b^{SM} \left\{ 1 - 3.57\delta g_L^b + 0.65\delta g_R^b \right\} \\ A_b &= \frac{(\delta \tilde{g}_L^b)^2 - (\delta \tilde{g}_R^b)^2}{(\delta \tilde{g}_L^b)^2 + (\delta \tilde{g}_R^b)^2} = A_b^{SM} \left\{ 1 - 0.31\delta g_L^b - 1.72\delta g_R^b \right\}, \end{aligned} \quad (7)$$

where R_b^{SM} and A_b^{SM} are the theory predictions including all radiative corrections. The positive contribution to $\delta g_L^{b,SM}$ from the top quark has the effect of reducing both R_b^{SM} and A_b^{SM} .

The 95% confidence level ellipse for new $Zb\bar{b}$ couplings is shown in Fig. 1 and is obtained

using the Particle Data Group results [37, 43]

$$\begin{aligned}
R_b^{exp} &= 0.21629 \pm 0.00066 \\
R_b^{SM} &= 0.21578 \pm 0.00005 \\
A_b^{exp} &= 0.923 \pm 0.020 \\
A_b^{SM} &= 0.9348 \pm 0.0001.
\end{aligned} \tag{8}$$

If $\delta g_R^b = 0$, the 95% confidence level limit from the fit to A_b and R_b is

$$-0.0027 < \delta g_L^b < 0.0014. \tag{9}$$

Similarly, if $\delta g_L^b = 0$, the 95% confidence level limit from the fit to A_b and R_b is

$$-0.0066 < \delta g_R^b < 0.0148. \tag{10}$$

B. Limits from the Oblique Parameters S , T and U

The new quarks contribute at loop level to the vacuum polarizations of the electroweak gauge bosons $\Pi_{XY}^{\mu\nu}(p^2) = \Pi_{XY}(p^2)g^{\mu\nu} + B_{XY}(p^2)p^\mu p^\nu$, with $XY = \gamma\gamma, \gamma Z, ZZ$ and W^+W^- [44, 45]. These effects can be parametrized using the S, T and U functions of Peskin and Takeuchi [44],

$$\begin{aligned}
\alpha S_F &= \frac{4s_W^2 c_W^2}{M_Z^2} \left\{ \Pi_{ZZ}(M_Z^2) - \Pi_{ZZ}(0) - \Pi_{\gamma\gamma}(M_Z^2) - \frac{c_W^2 - s_W^2}{c_W s_W} \Pi_{\gamma Z}(M_Z^2) \right\} \\
\alpha T_F &= \frac{\Pi_{WW}(0)}{M_W^2} - \frac{\Pi_{ZZ}(0)}{M_Z^2} \\
\alpha U_F &= 4s_W^2 \left\{ \frac{\Pi_{WW}(M_W^2) - \Pi_{WW}(0)}{M_W^2} - c_W^2 \left(\frac{\Pi_{ZZ}(M_Z^2) - \Pi_{ZZ}(0)}{M_Z^2} \right) \right. \\
&\quad \left. - 2s_W c_W \frac{\Pi_{\gamma Z}(M_Z^2)}{M_Z^2} - s_W^2 \frac{\Pi_{\gamma\gamma}(M_Z^2)}{M_Z^2} \right\}.
\end{aligned} \tag{11}$$

Any definition of s_W can be used in Eq. 11 since the scheme dependence enters at higher order. Since these parameters are well-constrained by LEP and LEP2 measurements [46], they set stringent limits on the masses and couplings of the new quarks.

We use the fit to the electroweak precision data given in Refs. [2, 47],

$$\begin{aligned}
\Delta S &= S - S_{SM} = 0.02 \pm 0.11 \\
\Delta T &= T - T_{SM} = 0.05 \pm 0.12 \\
\Delta U &= U - U_{SM} = 0.07 \pm 0.12,
\end{aligned} \tag{12}$$

with reference Higgs and top-quark masses $M_{H,\text{ref}} = 120$ GeV and $m_{t,\text{ref}} = 173.1$ GeV. The associated correlation matrix is

$$\rho_{ij} = \begin{pmatrix} 1.0 & 0.879 & -0.469 \\ 0.879 & 1.0 & -0.716 \\ -0.469 & -0.716 & 1.0 \end{pmatrix}.$$

The $\Delta\chi^2$ is defined as

$$\Delta\chi^2 = \sum_{i,j} (\Delta X_i - \Delta \hat{X}_i) (\sigma^2)_{ij}^{-1} (\Delta X_j - \Delta \hat{X}_j), \quad (13)$$

where $\Delta \hat{X}_i = \Delta S, \Delta T$ and ΔU are the central values of the fit in Eq. 12, $\Delta X_i = X_i - X_i^{SM} = \Delta S_F, \Delta T_F$ and ΔU_F are the contributions to the oblique parameters from the new fermions and $\sigma_{ij}^2 \equiv \sigma_i \rho_{ij} \sigma_j$, σ_i being the errors given in Eq. 12. A 95% confidence level limit in a three-parameter fit corresponds to $\Delta\chi^2 = 7.82$.

Since we consider primarily $M_H = 125$ GeV, we need to add the Higgs contributions¹

$$\begin{aligned} \Delta S_H &= \frac{1}{12\pi} \log\left(\frac{M_H^2}{M_{H,\text{ref}}^2}\right) + \mathcal{O}\left(\frac{M_Z^2}{M_H^2}\right) \\ \Delta T_H &= -\frac{3}{16\pi c_W^2} \log\left(\frac{M_H^2}{M_{H,\text{ref}}^2}\right) + \mathcal{O}\left(\frac{M_Z^2}{M_H^2}\right) \\ \Delta U_H &= \mathcal{O}\left(\frac{M_Z^2}{M_H^2}\right). \end{aligned} \quad (14)$$

C. Other Experimental Limits on Top Partner Models

Both ATLAS [50, 51] and CMS [52, 53] have searched for direct pair production of new heavy fermions. For charge 2/3 top-like quarks decaying with 100% branching ratio to Wb , CMS excludes masses below 557 GeV at 95% confidence level, while ATLAS sets an upper bound of 404 GeV. CMS dedicates a specific analysis to pair-produced vector quarks of charge 2/3 decaying entirely to Zt , excluding masses below 475 GeV [54]. For charge -1/3 quarks, assuming 100% branching ratio to Zb , ATLAS excludes masses below 358 GeV for a vector singlet, while CMS excludes charge -1/3 quarks decaying with 100% branching ratio to Wt below 611 GeV. These limits are not directly applicable to our models, since the

¹ Our fits include the exact results for the Higgs contributions, which can be found in many places including Ref. [48] and the Appendix of Ref. [49].

branching ratios of the new heavy fermions to Standard Model particles are degraded by mixing angles and the limits therefore weakened [36, 55–59]. Our results on Higgs production are rather insensitive to the masses of the new top partners and we typically assume masses of the TeV scale.

In principle, there are also limits on heavy charged fermions which mix with the Standard Model third generation quarks coming from K , B and D rare processes. For TeV-scale masses of the new fermions and small mixing parameters (which we will see in the next section are required by limits from oblique parameters, R_b and A_b), the constraints from rare processes are not restrictive [57, 59–61].

IV. SINGLET TOP PARTNER MODEL

Little Higgs models [17–23], topcolor models [24, 25] and top condensate models [26–28] all contain a charge 2/3 partner of the top quark, which we denote by \mathcal{T}^2 . We consider a general case with a vector $SU(2)_L$ singlet fermion which is allowed to mix with the Standard Model-like top quark [19, 36, 60, 62, 63]. The mass eigenstates are $b \equiv \tilde{\mathcal{B}}^1$, t and T , where b and t are the observed bottom and top quarks. Thorough this paper we will use the measured mass values $m_b = 4.19$ GeV, $m_t = 173.1$ GeV [37, 64]. The mass eigenstates of charge 2/3 can be found through the rotations

$$\chi_{L,R}^t \equiv \begin{pmatrix} t_{L,R} \\ T_{L,R} \end{pmatrix} \equiv U_{L,R}^t \begin{pmatrix} \mathcal{T}_{L,R}^1 \\ \mathcal{T}_{L,R}^2 \end{pmatrix}. \quad (15)$$

The matrices $U_{L,R}^t$ are unitary and $\Psi_{L,R} \equiv \frac{1 \mp \gamma_5}{2} \Psi$. The mixing matrices are parametrized as

$$U_L^t = \begin{pmatrix} \cos \theta_L & -\sin \theta_L \\ \sin \theta_L & \cos \theta_L \end{pmatrix}, \quad U_R^t = \begin{pmatrix} \cos \theta_R & -\sin \theta_R \\ \sin \theta_R & \cos \theta_R \end{pmatrix}. \quad (16)$$

We abbreviate $c_L \equiv \cos \theta_L$, $s_L \equiv \sin \theta_L$.

The most general fermion mass terms are

$$\begin{aligned} -\mathcal{L}_{M,1} &= -\mathcal{L}_M^{SM} + \lambda_3 \bar{\psi}_L^1 \tilde{H} \mathcal{T}_R^2 + \lambda_4 \bar{\mathcal{T}}_L^2 \mathcal{T}_R^1 + \lambda_5 \bar{\mathcal{T}}_L^2 \mathcal{T}_R^2 + \text{h.c.} \\ &= \bar{\chi}_L^t \left[U_L^t \left(M_{(1)}^t + h H_{(1)}^t \right) U_R^{t\dagger} \right] \chi_R^t + \lambda_1 \frac{v+h}{\sqrt{2}} \bar{\mathcal{B}}_L^1 \mathcal{B}_R^1 + \text{h.c.}, \end{aligned} \quad (17)$$

where

$$M_{(1)}^t = \begin{pmatrix} \lambda_2 \frac{v}{\sqrt{2}} & \lambda_3 \frac{v}{\sqrt{2}} \\ \lambda_4 & \lambda_5 \end{pmatrix}, \quad H_{(1)}^t = \frac{1}{\sqrt{2}} \begin{pmatrix} \lambda_2 & \lambda_3 \\ 0 & 0 \end{pmatrix}. \quad (18)$$

The resulting mass eigenstates are

$$\mathcal{M}^{t,diag} \equiv \begin{pmatrix} m_t & 0 \\ 0 & M_T \end{pmatrix}. \quad (19)$$

One can always rotate \mathcal{T}^2 such that $\lambda_4 = 0$. Since λ_4 can be rotated away, the model has four free parameters. Alternatively, it is always possible to rotate \mathcal{T}_R^2 such that $\sin \theta_R = 0$, because only the Standard Model-like left-handed doublet ψ_L^1 mixes to the singlet with a Yukawa term². Therefore the couplings only depend on θ_L , which we will take as one of the four physical parameters along with m_b (physical mass of the charge -1/3 quark), m_t and M_T (physical masses of the charge 2/3 quarks).

The physical masses and mixing angles are found using bi-unitary transformations,

$$\begin{aligned} \left(\mathcal{M}^{t,diag} \right)^2 &= U_L^t M_{(1)}^t M_{(1)}^{t,\dagger} U_L^{t,\dagger} \\ &= U_R^t M_{(1)}^{t,\dagger} M_{(1)}^t U_R^{t,\dagger}. \end{aligned} \quad (20)$$

It is straightforward to find the mass eigenstates and mixing angles,

$$\begin{aligned} \tan(2\theta_R) &= \frac{2\lambda_4\lambda_5 + v^2\lambda_2\lambda_3}{\lambda_5^2 - \lambda_4^2 + \frac{v^2}{2}(\lambda_3^2 - \lambda_2^2)} \\ \tan(2\theta_L) &= \frac{\sqrt{2}v(\lambda_2\lambda_4 + \lambda_3\lambda_5)}{\lambda_5^2 + \lambda_4^2 - \frac{v^2}{2}(\lambda_2^2 + \lambda_3^2)} \\ m_t M_T &= \frac{v}{\sqrt{2}} | \lambda_2\lambda_5 - \lambda_3\lambda_4 | \\ M_T^2 + m_t^2 &= \frac{v^2}{2}(\lambda_2^2 + \lambda_3^2) + \lambda_4^2 + \lambda_5^2. \end{aligned} \quad (21)$$

From Eq. 17, the couplings to the Higgs boson are

$$\mathcal{L}_1^h = -\frac{m_t}{v} c_{tt} \bar{t}_L t_R h - \frac{M_t}{v} c_{TT} \bar{T}_L T_R h - \frac{M_t}{v} c_{tT} \bar{t}_L T_R h - \frac{m_t}{v} c_{Tt} \bar{T}_L t_R h + \text{h.c.}, \quad (22)$$

where

$$c_{tt} = c_L^2, \quad c_{TT} = s_L^2, \quad c_{tT} = c_{Tt} = s_L c_L. \quad (23)$$

These relations can be easily derived by noticing that

$$v H_{(1),ks}^t = M_{(1),ks}^t \delta_{k1}, \quad (24)$$

² We do not perform any of these rotations here, and the formulas in this section hold for the arbitrary Yukawa couplings of Eq. 17.

yielding for the physical Higgs couplings

$$\begin{aligned}
H_{ij} &\equiv U_{L,ik}^t H_{(1),ks}^t U_{R,sj}^{t,\dagger} \\
&= v^{-1} U_{L,i\hat{k}}^t \delta_{\hat{k}1} \left[U_{L,\hat{k}r}^{t,\dagger} \mathcal{M}_{rr}^{t,diag} U_{R,rs}^t \right] U_{R,sj}^{t,\dagger} \\
&= v^{-1} U_{L,i\hat{k}}^t \delta_{\hat{k}1} U_{L,\hat{k}j}^{t,\dagger} \mathcal{M}_{jj}^{t,diag},
\end{aligned} \tag{25}$$

where the index \hat{k} is not summed over.

The charged and neutral current interactions are

$$\mathcal{L}_1^{CC} = \frac{g}{\sqrt{2}} W^{\mu+} \sum_{i=1,2} \left(\bar{\chi}_L^t \right)_i \left(U_L^t \right)_{i,1} \gamma_\mu b_L + \text{h.c.} \tag{26}$$

and

$$\begin{aligned}
\mathcal{L}_1^{NC} &= \frac{g}{c_W} Z_\mu \sum_{i=t,T} \left\{ \bar{f}_i \gamma^\mu \left[(g_L^i + \delta \tilde{g}_L^i) P_L + (g_R^i + \delta \tilde{g}_R^i) P_R \right] f_i \right\} \\
&\quad + \frac{g}{c_W} Z_\mu \sum_{i \neq j} \left\{ \bar{f}_i \gamma^\mu \left[\delta g_L^{ij} P_L + \delta g_R^{ij} P_R \right] f_j \right\},
\end{aligned} \tag{27}$$

where $\delta \tilde{g}_{L,R}^i = \delta g_{L,R}^{i,SM} + \delta g_{L,R}^i$ contains both the Standard Model contribution from top quark loops and the new physics contributions. The new physics couplings arising from the interactions of the top partner singlet are

$$\begin{aligned}
\delta g_L^t &= -\frac{s_L^2}{2}, \quad \delta g_L^T = -\frac{c_L^2}{2}, \quad \delta g_L^{tT} = \frac{s_L c_L}{2} \\
\delta g_R^i &= \delta g_R^{ij} = 0, \quad i, j = t, T.
\end{aligned} \tag{28}$$

Finally, the unitarity bound from the scattering $T\bar{T} \rightarrow T\bar{T}$ is modified from the Standard Model limit and becomes [65, 66]

$$M_T(\text{Unitarity Bound}) \lesssim \frac{550 \text{ GeV}}{s_L^2}. \tag{29}$$

This class of models therefore allows quite heavy T quarks without violating perturbative unitarity.

A. Experimental Restrictions on Singlet Top Partner Model

Using the results given above, it is straightforward to compute the contributions to the S, T and U parameters in the singlet top partner model. Expressions for the gauge boson

two-point functions for arbitrary fermion couplings are given in the appendix [21, 67, 68], and we assume $M_T \gg M_Z$. Subtracting the Standard Model $t-b$ loops, the new contributions are

$$\begin{aligned}
\Delta T_F &= T_{SM} s_L^2 \left[-(1 + c_L^2) + s_L^2 r + 2c_L^2 \frac{r}{r-1} \log(r) + \mathcal{O}\left(\frac{M_Z^2}{m_t^2}, \frac{M_Z^2}{M_T^2}, \frac{m_b^2}{m_t^2}\right) \right] \\
\Delta S_F &= -\frac{N_C}{18\pi} s_L^2 \left\{ \log(r) + c_L^2 \left[\frac{5(r^2 + 1) - 22r}{(r-1)^2} + \frac{3(r+1)(r^2 - 4r + 1)}{(1-r)^3} \log(r) \right] \right. \\
&\quad \left. + \mathcal{O}\left(\frac{M_Z^2}{m_t^2}, \frac{M_Z^2}{M_T^2}, \frac{m_b^2}{m_t^2}\right) \right\} \\
\Delta S_F + \Delta U_F &= \frac{N_C}{9\pi} s_L^2 \left[\log(r) + \mathcal{O}\left(\frac{M_Z^2}{m_t^2}, \frac{M_Z^2}{M_T^2}, \frac{m_b^2}{m_t^2}\right) \right], \tag{30}
\end{aligned}$$

where

$$r \equiv \frac{M_T^2}{m_t^2}, \quad N_C = 3, \quad \text{and} \quad T_{SM} = \frac{N_C}{16\pi s_W^2} \frac{m_t^2}{M_W^2} \tag{31}$$

is the $t-b$ contribution to the T parameter in the limit of a massless bottom quark. We use $M_W = 80.4$ GeV, $M_Z = 91.2$ GeV [37]. Eq. 30 agrees with the $m_b \rightarrow 0$ and $M_Z \ll M_T, m_t$ limits of Refs. [69–71].³ For a top partner much heavier than the top quark, $M_T \gg m_t$, the oblique parameters take simple forms,

$$\begin{aligned}
\Delta T_F(\text{approx}) &= T_{SM} s_L^2 \left[-(1 + c_L^2) + s_L^2 r + 2c_L^2 \log(r) \right] \\
\Delta S_F(\text{approx}) &= -\frac{N_C}{18\pi} s_L^2 \left[5c_L^2 + (1 - 3c_L^2) \log(r) \right]. \tag{32}
\end{aligned}$$

One would expect decoupling to occur for a very heavy vector top partner, i.e. for $r \rightarrow \infty$. From Eqs. 30, 32, instead, the effects of the top partner on the oblique parameters vanish only in the limit $s_L \rightarrow 0$. This can be understood inspecting the mass matrix (18): to obtain decoupling both the Yukawa interactions and the off-diagonal terms need to be small, $\lambda_2 v, \lambda_3 v, \lambda_4 \ll \lambda_5$. In this limit

$$s_L \rightarrow \frac{v\lambda_3}{\sqrt{2}M_T} + \frac{\lambda_2\lambda_4 v}{\sqrt{2}M_T^2} + \dots \tag{33}$$

and the top partner effects vanish for large M_T , as expected.

In Fig. 2 we show the oblique parameters for a fixed $M_T = 1$ TeV. It is clear that the approximate forms of Eq. 32 are excellent approximations to the complete results for mass

³ There is a typo in Eq. 88 of Ref. [70], where there is a 2 instead of the factor 22 in Eq. 30.

Singlet Fermion Model

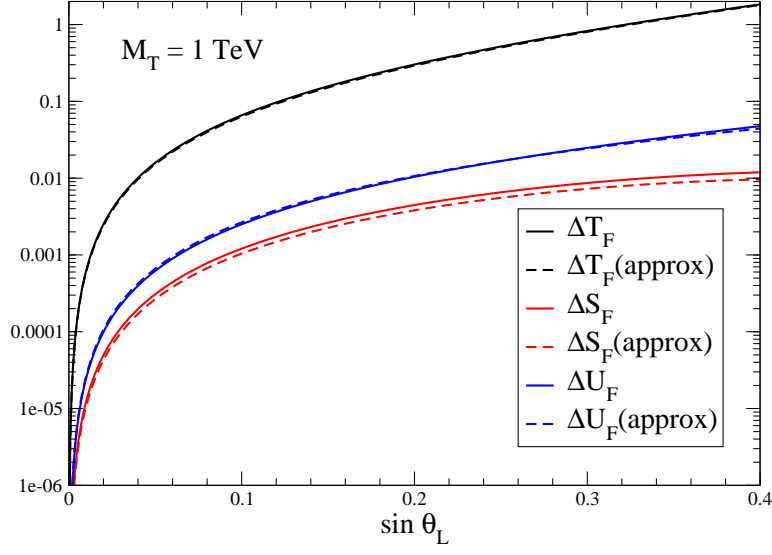


FIG. 2: Contributions to ΔT_F , ΔS_F , ΔU_F from a singlet top partner as a function of $\sin \theta_L$ for fixed $M_T = 1$ TeV. The results of Eq. 32 in the limit $M_T \gg m_t$ are shown as $\Delta T_F(\text{approx})$, $\Delta S_F(\text{approx})$ and $\Delta U_F(\text{approx})$.

Singlet Fermion Model

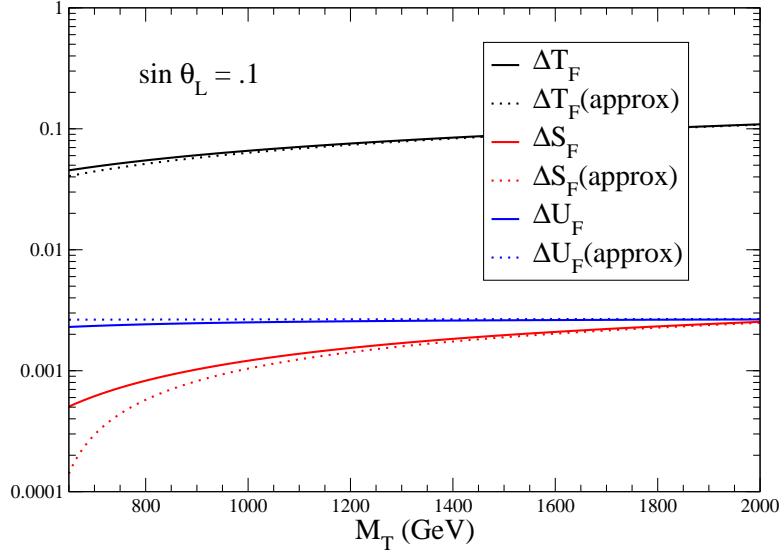


FIG. 3: Fermion contributions to ΔT_F , ΔS_F , ΔU_F in the singlet top partner model for fixed $\sin \theta_L = 0.1$. The dotted lines represent the approximate results from Eq. 32 in the limit $M_T \gg m_t$.

Singlet Fermion Model

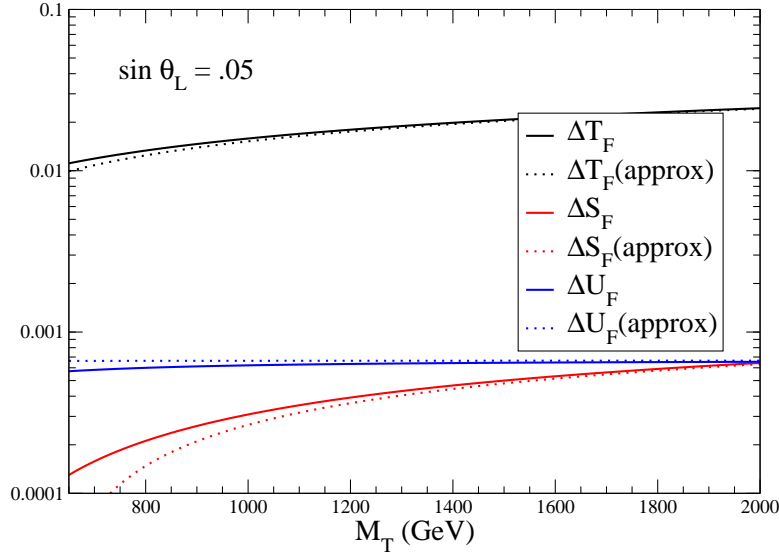


FIG. 4: Same as Fig. 3 for a smaller $\sin \theta_L = 0.05$.

values of this order. The largest contribution is to ΔT_F due to the large isospin violation for non-zero $\sin \theta_L$. In this case, the isospin violation is manifest in the result that $\Delta U_F > \Delta S_F$. The new physics effects vanish as $s_L \rightarrow 0$ and we recover the Standard Model couplings. The oblique parameters for fixed $\sin \theta_L$ are shown in Figs. 3 and 4 as a function of M_T . As we argued, the decoupling does not occur for large M_T , but requires $s_L \rightarrow 0$.

The parameter space allowed by a fit to the oblique parameters can be found using the results of Section III. Fig. 5 shows the 95% confidence level upper bound on the mixing angle $\sin \theta_L$ as a function of M_T for a light Higgs boson. For a heavier Higgs boson, it is possible to use the positive contribution to T from the top partner to compensate for the negative contribution from the heavy Higgs, as shown in Fig. 6. In this case, a minimum degree of mixing is required, since such a heavy Higgs boson is excluded by the electroweak fit in the three-generation Standard Model. The heavier the Higgs boson, the smaller the range of $\sin \theta_L$ allowed. This situation was explored for an extremely heavy Higgs boson ($M_H \sim 800$ GeV) in Ref. [72].

The mixing in the charge 2/3 sector also affects R_b . In the limit $m_b \rightarrow 0$ and neglecting the small correlations between R_b and the oblique parameters, only δg_L^b is affected by the singlet

95% Confidence Level Upper Bound from STU

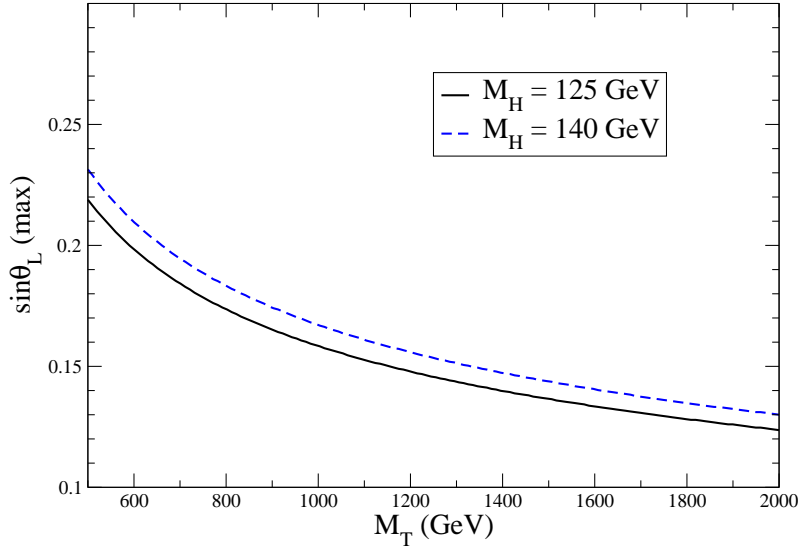


FIG. 5: 95% confidence level upper bound on the mixing angle $\sin \theta_L$ in the singlet top partner model from experimental restrictions on the S , T and U parameters.

95% Confidence Level Allowed Regions from STU
(Between Curves)

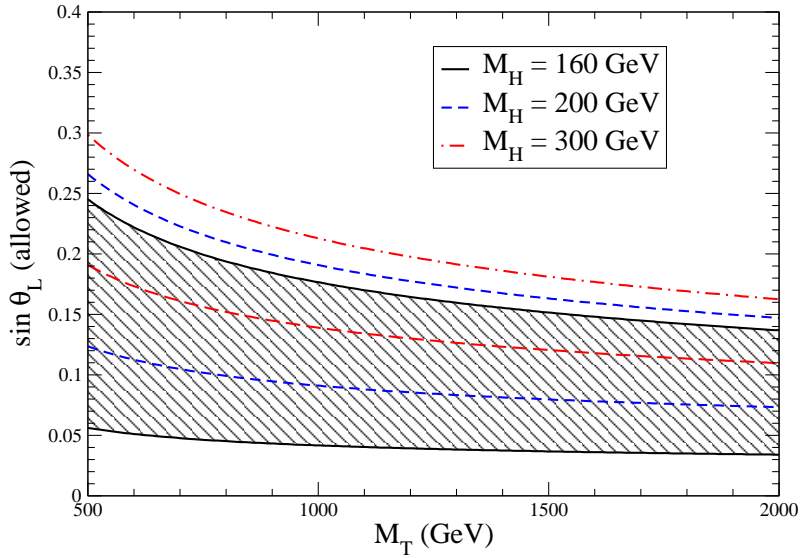


FIG. 6: 95% confidence level bands allowed by a fit to S , T and U for the mixing angle $\sin \theta_L$ in the singlet top partner model. The regions allowed are between the curves corresponding to each value of M_H .

top partner. Its contribution to δg_L^b can be found from the general analysis of Ref. [73],

$$\delta g_L^b = \frac{g^2}{64\pi^2} s_L^2 \left(f_1(x, x') + c_L^2 f_2(x, x') \right), \quad (34)$$

where $x = m_t^2/M_W^2$ and $x' = M_T^2/M_W^2$. The Standard Model top contribution has been subtracted following the definition of Eq. 5. In the heavy mass limit, $x, x' \gg 1$,

$$\begin{aligned} f_1(x, x') &= x' - x + 3 \log\left(\frac{x'}{x}\right) \\ f_2(x, x') &= -x - x' + \frac{2xx'}{x' - x} \log\left(\frac{x'}{x}\right). \end{aligned} \quad (35)$$

The contribution to δg_L^b from top singlet partners is shown in Fig. 7 as a function of M_T for fixed $\sin \theta_L$, along with the 95% confidence level region allowed from the fit of Section III A. We use the exact one-loop calculation of δg_L^b in the top singlet partner model, following Refs. [73, 74]. The relatively large contributions from R_b can be understood by looking at the leading terms for $m_t, M_T \gg M_W$,

$$\delta g_L^b = \delta g_L^{b,SM} s_L^2 \left[-(1 + c_L^2) + s_L^2 r + 2c_L^2 \frac{r}{r-1} \log(r) \right]. \quad (36)$$

Again we see that the heavy top partner decouples only when the parameters in the mass matrix are such that $s_L \sim \frac{v}{M_T}$. Furthermore, its contributions to δg_L^b and to the T parameter (Eq. 32) are both positive and strongly correlated. A large, positive contribution to δg_L^b from the singlet also implies a large contribution to the T parameter. This correlation was already pointed out in the context of composite Higgs models in Refs. [31, 32, 75].

Combining the new physics contribution with the Standard Model top quark contribution,

$$\delta \tilde{g}_L^b = \delta g_L^{b,SM} + \delta g_L^b = \delta g_L^{b,SM} \left[c_L^4 + s_L^4 r + 2s_L^2 c_L^2 \frac{r}{r-1} \log(r) \right], \quad (37)$$

and the net effect of the top partner is to increase $\delta \tilde{g}_L^b$ and hence reduce R_b .

A comparison of the maximum value of $\sin \theta_L$ allowed by the fit to R_b and A_b and by the experimental limits arising from the fit to S , T and U (with $M_H = 125$ GeV) is shown in Fig. 8, where it is apparent that the most stringent restrictions in the top partner singlet model come from the oblique parameters.

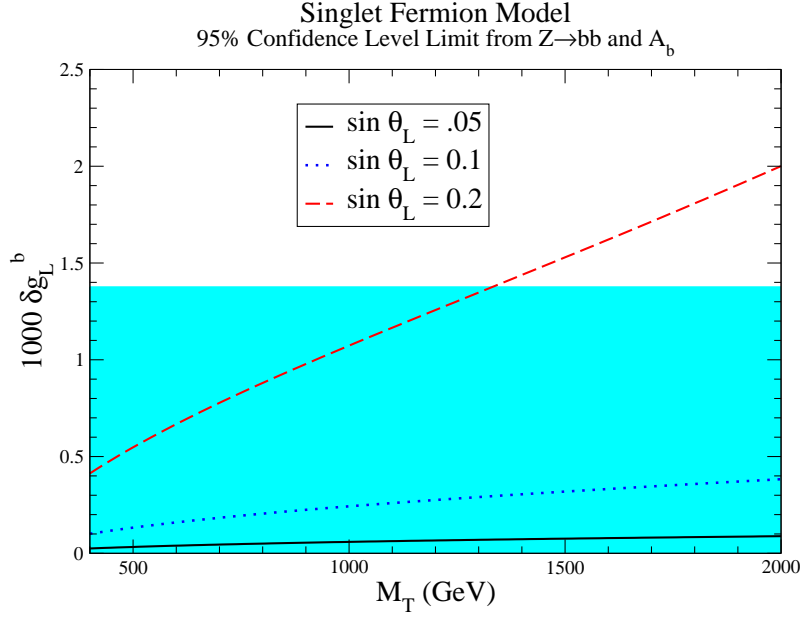


FIG. 7: Fermion contributions to δg_L^b as a function of M_T for fixed $\sin \theta_L$ in the top partner singlet model. The 95% confidence level allowed region is shaded in light blue.

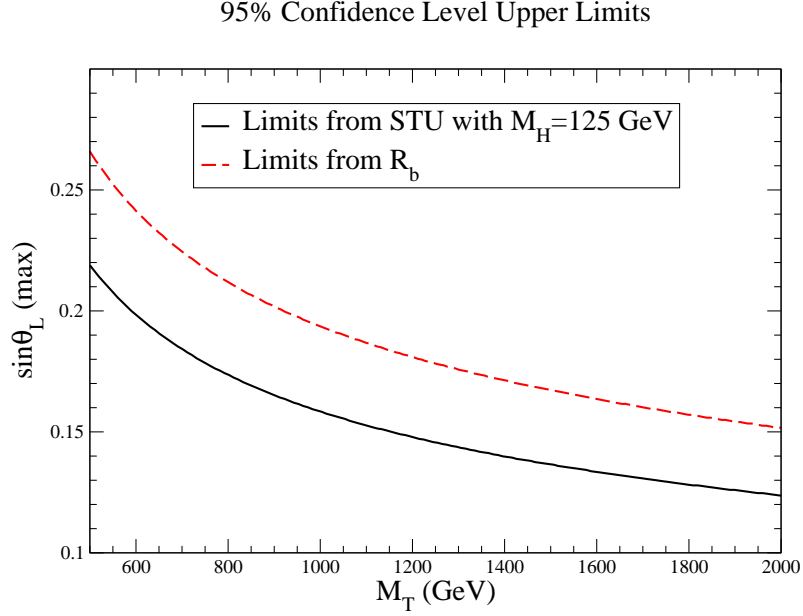


FIG. 8: Maximum allowed $\sin \theta_L$ in the top partner singlet model from oblique measurements (black solid) and R_b (red dashed).

V. TOP PARTNER DOUBLET

A. Model with Top Partner Doublet

In this section, we consider a model which has in addition to the Standard Model fields a vector $SU(2)_L$ doublet [36, 76],

$$\psi_L^2 = \begin{pmatrix} \mathcal{T}_L^2 \\ \mathcal{B}_L^2 \end{pmatrix}, \quad \psi_R^2 = \begin{pmatrix} \mathcal{T}_R^2 \\ \mathcal{B}_R^2 \end{pmatrix}. \quad (38)$$

The most general fermion mass terms allowed in the Lagrangian are

$$\begin{aligned} -\mathcal{L}_{M,2} &= -\mathcal{L}_M^{SM} + \lambda_6 \bar{\psi}_L^2 H \mathcal{B}_R^1 + \lambda_7 \bar{\psi}_L^2 \tilde{H} \mathcal{T}_R^1 + \lambda_8 \bar{\psi}_L^2 \psi_R^2 + \lambda_9 \bar{\psi}_L^1 \psi_R^2 + \text{h.c.} \\ &= \bar{\chi}_L^t \left[U_L^t M_{(2)}^t U_R^{t\dagger} \right] \chi_R^t + \bar{\chi}_L^b \left[U_L^b M_{(2)}^b U_R^{b\dagger} \right] \chi_R^b + \text{h.c.}, \end{aligned} \quad (39)$$

where $\chi_{L,R}^t$ are given by Eq. 15 and

$$\chi_{L,R}^b \equiv \begin{pmatrix} b_{L,R} \\ B_{L,R} \end{pmatrix} \equiv U_{L,R}^b \begin{pmatrix} \mathcal{B}_{L,R}^1 \\ \mathcal{B}_{L,R}^2 \end{pmatrix}. \quad (40)$$

We can always rotate ψ_2 such that $\lambda_9 = 0$. So without loss of generality

$$M_{(2)}^t = \begin{pmatrix} \lambda_2 \frac{v}{\sqrt{2}} & 0 \\ \lambda_7 \frac{v}{\sqrt{2}} & \lambda_8 \end{pmatrix}, \quad M_{(2)}^b = \begin{pmatrix} \lambda_1 \frac{v}{\sqrt{2}} & 0 \\ \lambda_6 \frac{v}{\sqrt{2}} & \lambda_8 \end{pmatrix}. \quad (41)$$

Because of the $SU(2)$ symmetry

$$M_{(2),22}^t = M_{(2),22}^b. \quad (42)$$

Diagonalizing the mass matrices now requires four unitary mixing matrices, $U_L^t, U_R^t, U_L^b, U_R^b$,

$$\begin{aligned} U_L^t &= \begin{pmatrix} \cos \theta_L^t & -\sin \theta_L^t \\ \sin \theta_L^t & \cos \theta_L^t \end{pmatrix}, & U_R^t &= \begin{pmatrix} \cos \theta_R^t & -\sin \theta_R^t \\ \sin \theta_R^t & \cos \theta_R^t \end{pmatrix}, \\ U_L^b &= \begin{pmatrix} \cos \theta_L^b & -\sin \theta_L^b \\ \sin \theta_L^b & \cos \theta_L^b \end{pmatrix}, & U_R^b &= \begin{pmatrix} \cos \theta_R^b & -\sin \theta_R^b \\ \sin \theta_R^b & \cos \theta_R^b \end{pmatrix}. \end{aligned} \quad (43)$$

There are five input parameters in the Lagrangian. We will take the five independent physical parameters to be the physical masses, m_t, M_T and m_b, M_B (with m_t and m_b being

the mass of the Standard Model-like fermions) and the right-handed mixing angle in the charge -1/3 sector, θ_R^b . It is straightforward to find relationships among the mixing angles:

$$\begin{aligned} (\sin \theta_R^t)^2 &= \frac{(\sin \theta_L^t)^2}{(\sin \theta_L^t)^2 + (\cos \theta_L^t)^2 \frac{m_t^2}{M_T^2}} \\ (\sin \theta_R^b)^2 &= \frac{(\sin \theta_L^b)^2}{(\sin \theta_L^b)^2 + (\cos \theta_L^b)^2 \frac{m_b^2}{M_B^2}} \\ (\sin \theta_R^b)^2 (m_b^2 - M_B^2) + M_B^2 &= (\sin \theta_R^t)^2 (m_t^2 - M_T^2) + M_T^2. \end{aligned} \quad (44)$$

For small mixing, the left-handed angles are always suppressed by the heavy mass scale relative to the right-handed angles of the same charge sector,

$$\sin^2 \theta_L^{t,b} \sim \frac{m_{t,b}^2}{M_{T,B}^2} \sin^2 \theta_R^{t,b}. \quad (45)$$

If the mass splitting between B and T , $\delta \equiv M_T - M_B$, is small, $\frac{|\delta|}{M_T} \ll 1$,

$$(\sin \theta_R^t)^2 = (\sin \theta_R^b)^2 + (\cos \theta_R^b)^2 \frac{2\delta}{M_T} + \mathcal{O}\left(\frac{\delta^2}{M_T^2}, \frac{m_t^2}{M_T^2}, \frac{m_b^2}{M_T^2}\right). \quad (46)$$

The charged current interactions are

$$\begin{aligned} \mathcal{L}_2^{CC} &= \frac{g}{\sqrt{2}} W^{\mu+} \left\{ \left[\Sigma_{i=1}^2 \bar{\psi}_L^i \gamma_\mu \sigma^- \psi_L^i \right] + \bar{\psi}_R^2 \gamma_\mu \sigma^- \psi_R^2 \right\} + \text{h.c.} \\ &= \frac{g}{\sqrt{2}} W^{\mu+} \left\{ \bar{\chi}_L^t \gamma_\mu U_L^t U_L^{b,\dagger} \chi_L^b + \bar{\chi}_R^t \gamma_\mu U_R^t U_R^{b,\dagger} \chi_R^b \right\} + \text{h.c.}, \end{aligned} \quad (47)$$

where

$$\sigma^- = \begin{pmatrix} 0 & 1 \\ 0 & 0 \end{pmatrix}. \quad (48)$$

The neutral current interactions are given by Eq. 27, with

$$\begin{aligned} \delta g_L^i &= \delta g_L^{ij} = 0, & i, j &= t, T, b, B \\ \delta g_R^t &= T_3^t \sin^2 \theta_R^t, & \delta g_R^T &= T_3^T \cos^2 \theta_R^t, & \delta g_R^{tT} &= -\frac{1}{2} \sin \theta_R^t \cos \theta_R^t \\ \delta g_R^b &= T_3^b \sin^2 \theta_R^b, & \delta g_R^B &= T_3^b \cos^2 \theta_R^b, & \delta g_R^{bB} &= \frac{1}{2} \sin \theta_R^b \cos \theta_R^b. \end{aligned} \quad (49)$$

In the doublet top-partner model, only the right-handed Standard Model-like singlets \mathcal{T}_1^R , \mathcal{B}_1^R have Yukawa type mixing with the new quarks, and therefore only the interactions in the right-handed sector are modified. Finally, the Higgs couplings are given by

$$\begin{aligned} \mathcal{L}_2^h &= -c_{tt} \frac{m_t}{v} \bar{t}_L t_R h - c_{TT} \frac{M_T}{v} \bar{T}_L T_R h - c_{tT} \frac{m_t}{v} \bar{t}_L T_R h - c_{Tt} \frac{M_T}{v} \bar{T}_L t_R h + \\ &\quad -c_{bb} \frac{m_b}{v} \bar{b}_L b_R h - c_{BB} \frac{M_B}{v} \bar{B}_L B_R h - c_{bB} \frac{m_b}{v} \bar{b}_L B_R h - c_{Bb} \frac{M_B}{v} \bar{B}_L b_R h + \text{h.c.}, \end{aligned} \quad (50)$$

where

$$\begin{aligned} c_{tt} &= \cos^2 \theta_R^t, & c_{TT} &= \sin^2 \theta_R^t, & c_{tT} &= c_{Tt} = \sin \theta_R^t \cos \theta_R^t \\ c_{bb} &= \cos^2 \theta_R^b, & c_{BB} &= \sin^2 \theta_R^b, & c_{bB} &= c_{Bb} = \sin \theta_R^b \cos \theta_R^b. \end{aligned} \quad (51)$$

The derivation of these couplings follows the lines of Eq. 25, just with

$$v H_{(2),ks}^t = M_{(1),ks}^t \delta_{s1}. \quad (52)$$

B. Experimental Limits on Doublet Fermion Model

The decay $Z \rightarrow b\bar{b}$ puts a strong restriction on $\sin \theta_b^R$ since mixing in the right-handed b -quark sector contributes to δg_R^b at tree level,

$$\delta g_R^b = -\frac{1}{2}(\sin \theta_R^b)^2. \quad (53)$$

From Eq. 10, the mixing angle in the right-handed b sector is highly constrained,

$$|\sin \theta_R^b| < 0.115. \quad (54)$$

The contribution to δg_L^b in the left-handed sector occurs at one-loop. Subtracting out the Standard Model contribution, in the limit $x, x' \gg 1$, the approximate result in the doublet fermion model is [34]

$$\delta g_L^b = \frac{g^2}{64\pi^2} \left\{ \sin^2(\theta_L^t - \theta_L^b) f_1(x, x') + (\sin \theta_R^t)^2 \cos^2(\theta_L^t - \theta_L^b) f_3(x, x') \right\}, \quad (55)$$

where $f_1(x, x')$ is defined in Eq. 35 and

$$f_3(x, x') = -x + \frac{3}{2} \left(1 + \frac{x}{x'} \right) + \left(\frac{x' + x}{2} - 3 \right) \frac{x}{(x' - x)} \log \left(\frac{x'}{x} \right). \quad (56)$$

In Fig. 9, we scan over $\sin \theta_R^b$ and $\frac{\delta}{M_T}$ and use the relationships of Eq. 44 to find the remaining parameters. We use the exact one-loop result for δg_b^L following Refs. [34, 74], and determine the 95% confidence level upper bound on $\frac{\delta}{M_T}$. Because of the tree level mixing in the b sector in this model, along with the relationships of Eq. 44, the heavy fermions are required to be approximately degenerate, as is clear from Fig. 9. This result is relatively insensitive to M_T .

Since $\sin \theta_R^b$ is constrained to be quite small, we will consider the oblique parameters in the limit $\theta_R^b = 0$. From Eq. 44, $\theta_R^b = 0$ implies $\theta_L^b = 0$ and the free parameters are m_t, m_b ,

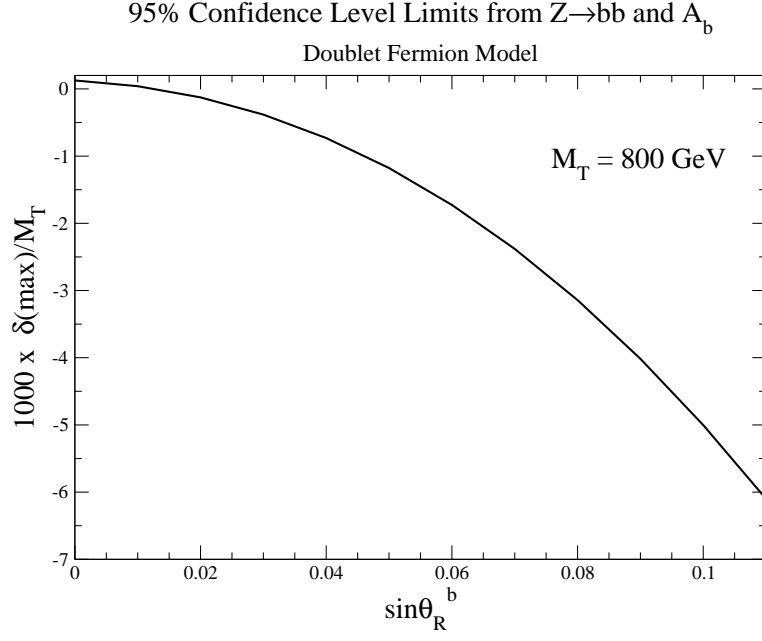


FIG. 9: Maximum value of $\frac{\delta}{M_T}$ allowed at the 95% confidence level from R_b and A_b as a function of $\sin \theta_R^b$ in the doublet fermion model.

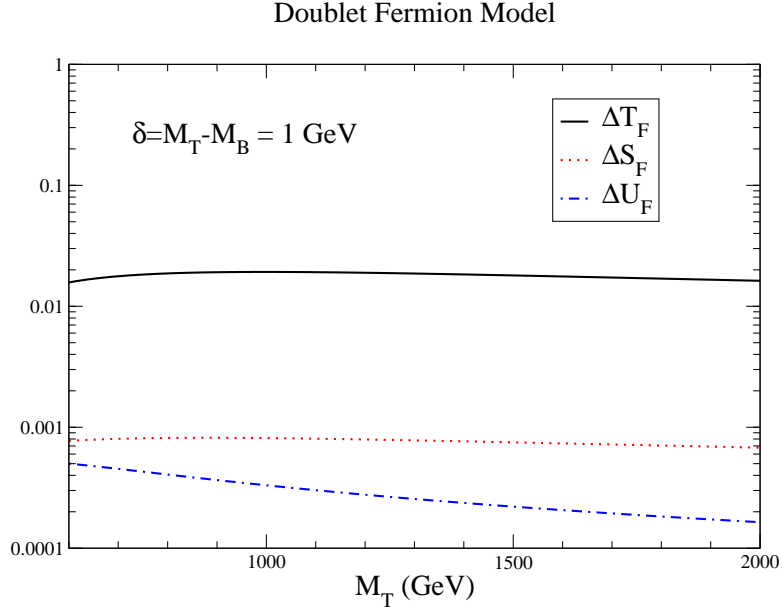


FIG. 10: Oblique parameters in the doublet fermion model in the limit $\theta_R^b = 0$ and $m_b \rightarrow 0$ as a function of M_T . We fix $\delta = M_T - M_B = 1 \text{ GeV}$.

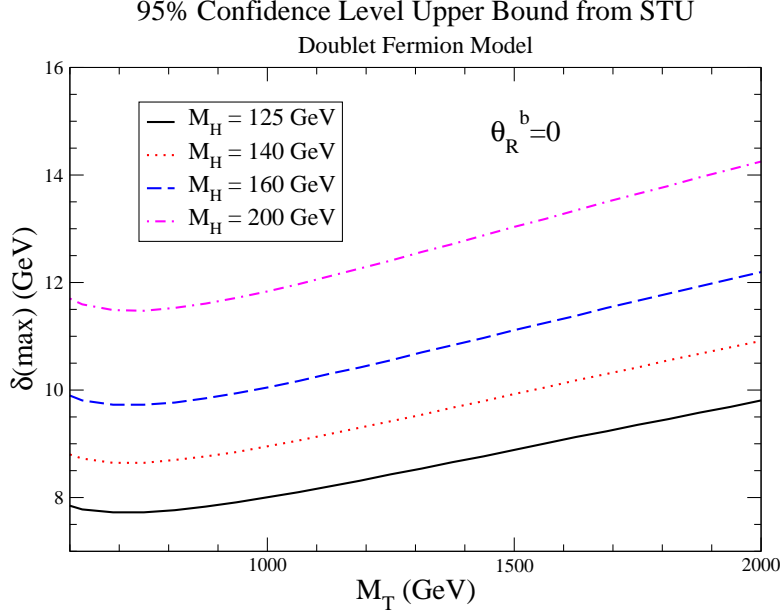


FIG. 11: Maximum mass splitting $\delta = M_T - M_B$ as a function of M_T allowed at the 95% confidence level from the oblique parameters in the doublet fermion model for $\theta_R^b = 0$.

M_T and M_B . Our results will always be expressed in terms of $\delta \equiv M_T - M_B$. In the $\theta_R^b = 0, m_b \rightarrow 0$ limit, the oblique parameters are well approximated by [69, 76]

$$\begin{aligned}\Delta T_F(\text{approx}) &= 4 T_{SM} \frac{\delta}{M_T} \left[2 \log(r) - 3 + \frac{5 \log(r) - 3}{r} \right] \\ \Delta S_F(\text{approx}) &= \frac{N_C}{9\pi} \frac{\delta}{M_T} \left[4 \log(r) - 7 + \frac{4 \log(r) + 7}{r} \right] \\ \Delta U_F(\text{approx}) &= \frac{N_C}{9\pi} \frac{\delta}{M_T} \left[3 + \frac{6 \log(r) - 17}{r} \right],\end{aligned}\tag{57}$$

and

$$\delta g_b^L = \delta g_b^{L,SM} \frac{\delta}{M_T} \left[\log(r) - 4 + 3 \frac{\log(r) - 2}{r} \right].\tag{58}$$

It is apparent that decoupling of the effects of the new fermions occurs in the isospin conserving limit, $\frac{\delta}{M_T} \rightarrow 0$. Note also that δg_b^L changes sign for $M_T \simeq 7m_t$. The oblique parameters are shown in Fig. 10 for $\delta = 1$ GeV. As in the singlet model, $\Delta T_F \gg \Delta S_F, \Delta U_F$.

The limits coming from the oblique parameters are found from a global fit to S , T and U as described in Section III B. For $\theta_R^b = 0$, the 95% upper limit on the mass splitting, δ , is shown in Fig. 11 as a function of M_T . For $M_H = 125$ GeV and $M_T \sim 1$ TeV, the experimental constraints on the oblique parameters require $\delta \lesssim 8$ GeV. As shown in Fig. 11, it is possible

to compensate for the negative contribution to T from a heavier Higgs boson by a larger mass splitting δ , which generates a positive contribution to ΔT_F . However, the limits from A_b and R_b in this model are much more stringent than those coming from the oblique parameters.

VI. PHENOMENOLOGY

The new fermions affect the gluon fusion production rate, which at lowest order is given by [77–79]

$$\sigma(gg \rightarrow H) = \frac{\alpha_s^2}{1024\pi v^2} \left| \sum_q c_{qq} F_{1/2}(\tau_q) \right|^2 \delta \left(1 - \frac{\hat{s}}{M_H^2} \right). \quad (59)$$

The sum is over t, b, T in the singlet fermion model and over t, b, T, B in the doublet model, the Yukawa couplings normalized to the Standard Model values c_{qq} are given in Eqs. 23 and 51, and

$$\begin{aligned} \tau_q &= \frac{4M_q^2}{M_H^2} \\ F_{1/2} &= -2\tau_q \left[1 + (1 - \tau_q)f(\tau_q) \right] \\ f(\tau_q) &= \begin{cases} \left[\sin^{-1} \left(\sqrt{\frac{1}{\tau_q}} \right) \right]^2, & \text{if } \tau_q \geq 1 \\ -\frac{1}{4} \left[\log \left(\frac{1 + \sqrt{1 - \tau_q}}{1 - \sqrt{1 - \tau_q}} - i\pi \right) \right]^2, & \text{if } \tau_q < 1. \end{cases} \end{aligned} \quad (60)$$

We compute the gluon fusion production cross section through NNLO using the program `iHixs` [8]. `iHixs` allows the calculation of the cross section at NNLO for extensions of the Standard Model with an arbitrary number of heavy quarks having non-standard Yukawa interactions [13], and puts the predictions on a firm theoretical basis. At NNLO, there are contributions which mix quark loops of different flavors (e.g. t and T) and cannot be obtained by a simple rescaling of the lowest order cross section. We scan the parameter space allowed by the precision electroweak data as determined in the previous sections and discuss the maximum deviations from the Standard Model predictions.

A. Top Partner Singlet Model

The deviation from the Standard Model prediction of the NNLO Higgs production cross section as a function of the mixing angle in the top partner singlet model is shown in

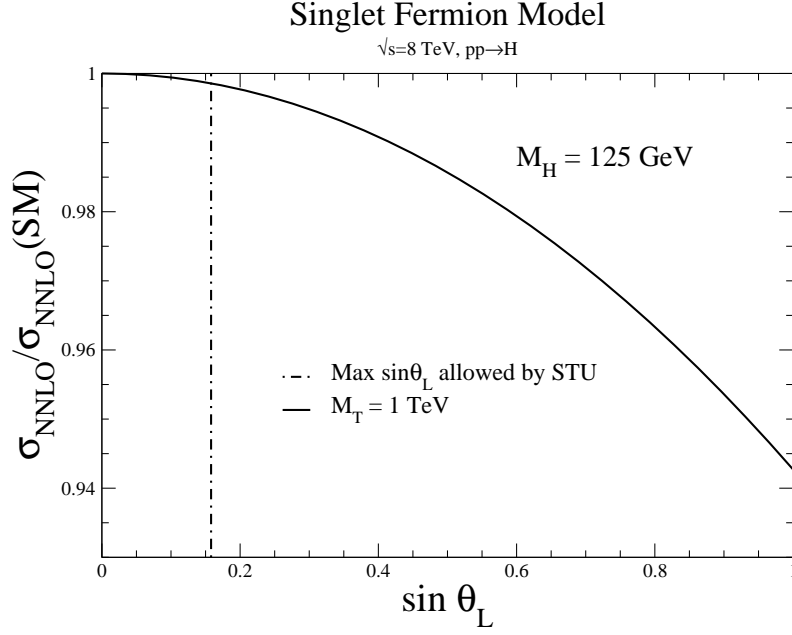


FIG. 12: The ratio of the NNLO Higgs cross section in the top partner singlet model normalized to the Standard Model prediction as a function of $\sin \theta_L$ for $M_H = 125$ GeV and $\sqrt{s} = 8$ TeV. The vertical line represents the maximum value of $\sin \theta_L$ allowed by electroweak precision measurements.

Fig. 12. The largest value of $\sin \theta_L$ allowed by the precision electroweak limits derived in Section IV A is also shown. As $\sin \theta_L$ increases, the mixing with the Standard Model-like top quark becomes significant, causing a suppression of the rate. This can be understood from the heavy mass limit ($m_t, M_T \gg \frac{M_H}{2}$) of the lowest order cross section, where the gluon fusion rate scales as

$$\frac{\sigma_{\text{Singlet}}}{\sigma_{\text{SM}}} \sim 1 - \frac{7}{60} \frac{M_H^2}{m_t^2} s_L^2 \left(1 - \frac{m_t^2}{M_T^2} \right). \quad (61)$$

However, only the region to the left of the dot-dash line in Fig. 12 is allowed by the precision electroweak measurements, making the Higgs boson production rate in this model almost identical to the Standard Model rate. In contrast with composite [80] or Little Higgs [59, 81] models, which typically have a sizeable reduction of the Higgs production cross section relative to the Standard Model, in models with vector fermions the suppression is negligible because of the decoupling properties discussed in the previous sections. The uncertainty on the Standard Model cross section coming from scale, PDF, and α_s uncertainties is roughly 15 – 20% [7], so the extremely small deviation from the Standard Model prediction in the top partner singlet model is unobservable. The cross section for a heavier Higgs boson of

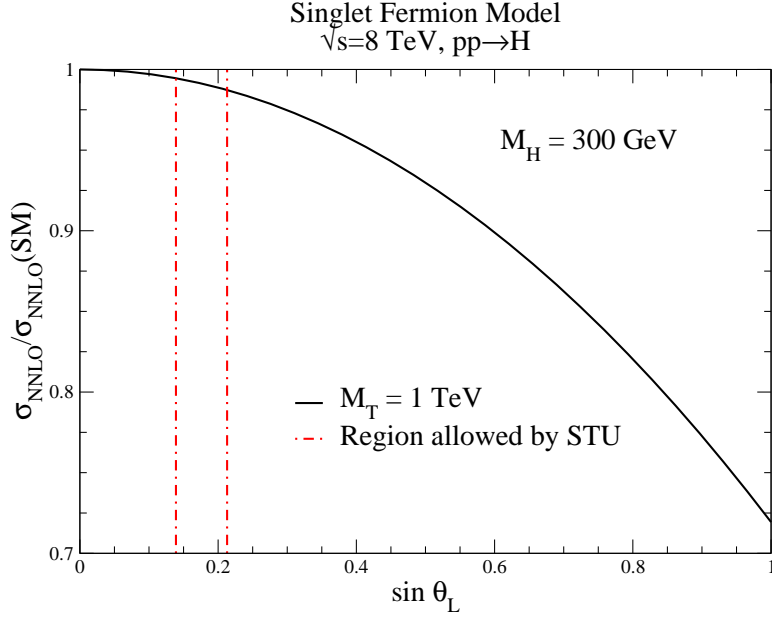


FIG. 13: The ratio of the NNLO Higgs cross section in the top partner singlet model normalized to the Standard Model prediction as a function of $\sin \theta_L$ for $M_H = 300$ GeV and $\sqrt{s} = 8$ TeV. The region between the vertical lines represents the region of $\sin \theta_L$ allowed by electroweak precision measurements.

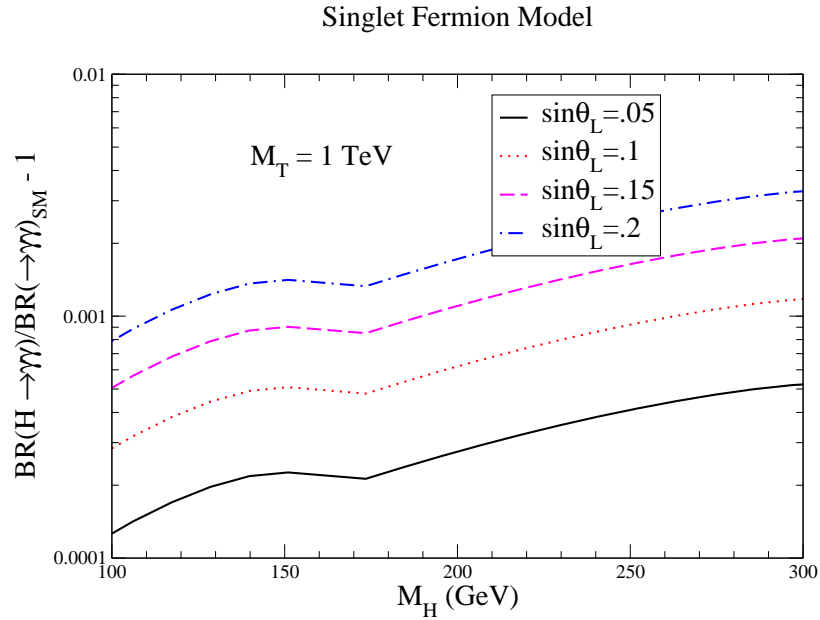


FIG. 14: Deviation of the $H \rightarrow \gamma\gamma$ branching ratio in the top partner singlet model from the Standard Model prediction.

mass $M_H = 300$ GeV is shown in Fig. 13. In this case, there is a region of mixing angles, $\sin \theta_L$, which is allowed by the precision electroweak measurements. Again, there is a slight, but unobservable, suppression of the NNLO rate relative to the Standard Model rate.

The loop-mediated Higgs decays to $\gamma\gamma$, $Z\gamma$ and gg are also affected by the presence of top fermion partners. Fig. 14 shows the deviation of the branching ratio to $\gamma\gamma$ from the Standard Model prediction. For small mixing, this deviation is always less than one percent.

B. Top Partner Doublet Model

The deviation from the Standard Model prediction for the NNLO gluon fusion cross section for Higgs production in the top partner doublet model (computed using iHixs) is shown in Fig. 15. Also in this case the maximum difference from the Standard Model in the allowed regions of parameter space (Fig. 9) is always less than a few percent. This result can be understood by considering the heavy mass limit of the lowest order cross section for

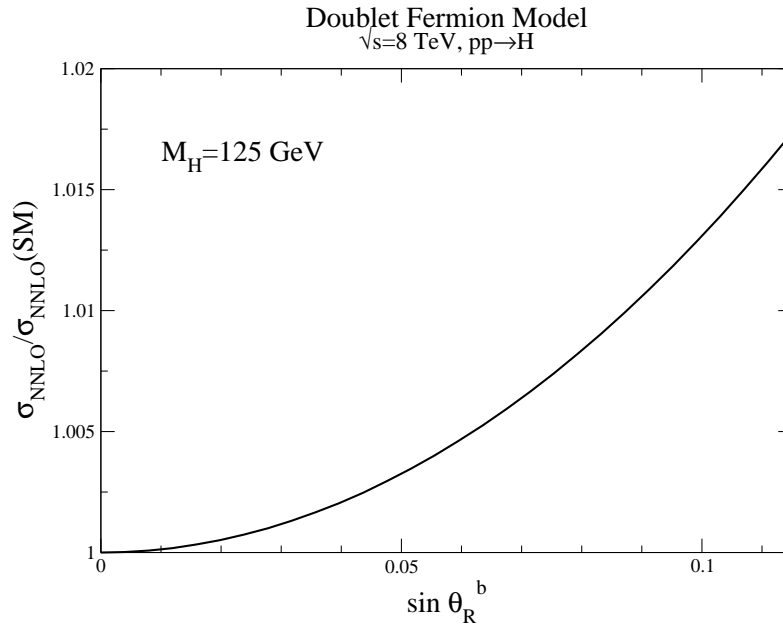


FIG. 15: The ratio of the NNLO Higgs cross section in the top partner doublet model normalized to the Standard Model prediction as a function of $\sin \theta_R^b$ for $M_H = 125$ GeV, $\sqrt{s} = 8$ TeV, and $M_T = M_B = 1$ TeV.

the gluon fusion production of the Higgs,

$$\frac{\sigma_{\text{Doublet}}}{\sigma_{SM}} \simeq \left(1 + \sin^2 \theta_R^b\right) \left[1 + \sin^2 \theta_R^b - \frac{7}{60} \frac{M_H^2}{m_t^2} \left(\frac{2r-1}{r} \sin^2 \theta_R^b + \frac{2\delta}{M_T} - \frac{2\delta}{M_T} \frac{r+1}{r} \sin^2 \theta_R^b\right)\right]. \quad (62)$$

From the fits to A_b and R_b , the maximum value of $\sin \theta_R^b$ is restricted to be 0.115, which implies

$$\frac{\sigma_{\text{Doublet}}}{\sigma_{SM}} \lesssim \left(1 + \sin^2 \theta_R^b\right)^2 \simeq 1.03. \quad (63)$$

Similarly, the deviations from the Standard Model in the Higgs decays to $\gamma\gamma$, $Z\gamma$ and gg and in $H \rightarrow b\bar{b}$, which is affected at tree level, are not observable due to the small mixings and mass splitting allowed.

VII. CONCLUSIONS

We have considered the effects on the gluon fusion Higgs boson production at NNLO from heavy vector quarks of charge 2/3 and -1/3. Since the new quarks are vector-like, their couplings to the Higgs boson are suppressed by mixing angles relative to the Standard Model Yukawa couplings. These mixing angles are restricted to be small by precision electroweak measurements. The most stringent bounds come from the oblique parameters for a vector singlet top-partner, and from A_b and R_b for an extension of the Standard Model with an additional vector doublet. Because of the small mixing angles allowed, in these models the Higgs boson production rate as well as its decay branching ratios are essentially those of the Standard Model. The scenarios we have presented will be extremely difficult to disentangle from the Standard Model without the observation of direct production of the heavy fermions. Vector doublet fermions with a non-standard hypercharge assignment are less restricted by precision electroweak measurements [36] and the mixing angles between the $t-b$ sector and the new fermion sector can be larger than in the cases we considered. However, even in this case, the low energy theorems for Higgs production require that the Higgs cross section approach the Standard Model result for large fermion masses.

If a Higgs boson is found at the LHC, attention will turn to understanding its properties. By performing global fits to the measured rates, information can be gleaned from the various cross section times branching ratio channels. For a light Higgs boson, it is likely that the

dominant production channel will be gluon fusion, even in models with new physics. In this case, the rates are sensitive not only to a rescaling of the Standard Model couplings, but also to the effects of new particles which couple to the Higgs boson and contribute to the decay rates. Numerous preliminary attempts have been made to use current LHC data to discern differences from the Standard Model [81–90]. Our scenario with vector fermions demonstrates the difficulty of these indirect determinations of new physics – it is (un)fortunately not difficult to construct models which give Higgs signals indistinguishable from the Standard Model.

Acknowledgements

We would like to thank G. Panico for useful discussions. This work is supported by the United States Department of Energy under Grant DE-AC02-98CH10886.

Appendix: Two Point Function for Arbitrary Fermion Coupling

The contributions to the gauge boson two point functions from fermion loops parametrized by the interaction

$$\mathcal{L} = \bar{f}_1 \left(C_{LX}^{f_1 f_2} P_L + C_{RX}^{f_1 f_2} P_R \right) \gamma_\mu f_2 V^\mu, \quad (64)$$

for $V = W, Z, \gamma$ are [21, 67]

$$\begin{aligned} \Pi_{XY} = & -\frac{N_c}{16\pi^2} \left\{ \frac{2}{3} \left(C_{LX}^{f_1 f_2} C_{LY}^{f_1 f_2} + C_{RX}^{f_1 f_2} C_{RY}^{f_1 f_2} \right) \left[m_1^2 + m_2^2 - \frac{p^2}{3} - \left(A_0(m_1) + A_0(m_2) \right) \right] \right. \\ & + \frac{m_1^2 - m_2^2}{2p^2} \left(A_0(m_1) - A_0(m_2) \right) + \frac{2p^4 - p^2(m_1^2 + m_2^2) - (m_1^2 - m_2^2)^2}{2p^2} B_0(m_1, m_2, p^2) \Big] \\ & \left. + 2m_1 m_2 \left(C_{LX}^{f_1 f_2} C_{RY}^{f_1 f_2} + C_{RX}^{f_1 f_2} C_{LY}^{f_1 f_2} \right) B_0(m_1, m_2, p^2) \right\} \end{aligned} \quad (65)$$

where

$$\begin{aligned} A_0(m) &= \left(\frac{4\pi\mu^2}{m^2} \right)^\epsilon \Gamma(1+\epsilon) \left(\frac{1}{\epsilon} + 1 \right) m^2 \\ B_0(m_1, m_2, p^2) &= \left(\frac{4\pi\mu^2}{m_2^2} \right)^\epsilon \Gamma(1+\epsilon) \left[\frac{1}{\epsilon} - f_1(m_1, m_2, p^2) \right] \end{aligned} \quad (66)$$

and

$$f_1(m_1, m_2, p^2) = \int_0^1 dx \log \left(x + \frac{m_1^2(1-x) - p^2 x(1-x)}{m_2^2} \right). \quad (67)$$

-
- [1] A.B. Arbuzov, M. Awramik, M. Czakon, A. Freitas, M.W. Grunewald, et al. ZFITTER: A Semi-analytical program for fermion pair production in e^+e^- annihilation, from version 6.21 to version 6.42. *Comput.Phys.Commun.*, 174:728–758, 2006.
 - [2] Henning Flacher et al. Revisiting the Global Electroweak Fit of the Standard Model and Beyond with Gfit. *Eur. Phys. J.*, C60:543–583, 2009.
 - [3] Serguei Chatrchyan et al. Combined results of searches for the standard model Higgs boson in pp collisions at $\sqrt{s} = 7$ TeV. *Phys.Lett.*, B710:26–48, 2012.
 - [4] Georges Aad et al. Combined search for the Standard Model Higgs boson using up to 4.9 fb-1 of pp collision data at $\sqrt{s} = 7$ TeV with the ATLAS detector at the LHC. *Phys.Lett.*, B710:49–66, 2012.
 - [5] Charalampos Anastasiou, Kirill Melnikov, and Frank Petriello. Higgs boson production at hadron colliders: Differential cross sections through next-to-next-to-leading order. *Phys. Rev. Lett.*, 93:262002, 2004.
 - [6] Robert V. Harlander and William B. Kilgore. Next-to-next-to-leading order Higgs production at hadron colliders. *Phys. Rev. Lett.*, 88:201801, 2002.
 - [7] LHC Higgs Cross Section Working Group, S. Dittmaier, C. Mariotti, G. Passarino, and R. Tanaka (Eds.). Handbook of LHC Higgs Cross Sections: 1. Inclusive Observables. *CERN-2011-002*, CERN, Geneva, 2011.
 - [8] Charalampos Anastasiou, Stephan Buehler, Franz Herzog, and Achilleas Lazopoulos. Total cross-section for Higgs boson hadroproduction with anomalous Standard Model interactions. *JHEP*, 12:058, 2011.
 - [9] Daniel de Florian and Massimiliano Grazzini. Higgs production through gluon fusion: Updated cross sections at the Tevatron and the LHC. *Phys.Lett.*, B674:291–294, 2009.
 - [10] Charalampos Anastasiou, Radja Boughezal, and Frank Petriello. Mixed QCD-electroweak corrections to Higgs boson production in gluon fusion. *JHEP*, 0904:003, 2009.
 - [11] Charalampos Anastasiou, Radja Boughezal, and Elisabetta Furlan. The NNLO gluon fusion Higgs production cross-section with many heavy quarks. *JHEP*, 06:101, 2010.
 - [12] Charalampos Anastasiou, Stephan Buehler, Elisabetta Furlan, Franz Herzog, and Achilleas

- Lazopoulos. Higgs production cross-section in a Standard Model with four generations at the LHC. *Phys. Lett.*, B702:224–227, 2011.
- [13] Elisabetta Furlan. Gluon-fusion Higgs production at NNLO for a non-standard Higgs sector. *JHEP*, 10:115, 2011.
 - [14] Graham D. Kribs, Tilman Plehn, Michael Spannowsky, and Timothy M.P. Tait. Four generations and Higgs physics. *Phys.Rev.*, D76:075016, 2007.
 - [15] Otto Eberhardt, Alexander Lenz, and Jurgen Rohrwild. Less space for a new family of fermions. *Phys.Rev.*, D82:095006, 2010.
 - [16] The CMS collaboration. Combined results of searches for a Higgs boson in the context of the Standard Model and Beyond-Standard Models.
 - [17] N. Arkani-Hamed, A.G. Cohen, E. Katz, and A.E. Nelson. The Littlest Higgs. *JHEP*, 0207:034, 2002.
 - [18] Ian Low, Witold Skiba, and David Tucker-Smith. Little Higgses from an antisymmetric condensate. *Phys.Rev.*, D66:072001, 2002.
 - [19] Maxim Perelstein, Michael E. Peskin, and Aaron Pierce. Top quarks and electroweak symmetry breaking in little Higgs models. *Phys.Rev.*, D69:075002, 2004.
 - [20] Spencer Chang and Jay G. Wacker. Little Higgs and custodial SU(2). *Phys.Rev.*, D69:035002, 2004.
 - [21] Mu-Chun Chen and Sally Dawson. One loop radiative corrections to the rho parameter in the littlest Higgs model. *Phys.Rev.*, D70:015003, 2004.
 - [22] Jay Hubisz, Patrick Meade, Andrew Noble, and Maxim Perelstein. Electroweak precision constraints on the littlest Higgs model with T parity. *JHEP*, 0601:135, 2006.
 - [23] Tao Han, Heather E. Logan, and Lian-Tao Wang. Smoking-gun signatures of little Higgs models. *JHEP*, 0601:099, 2006.
 - [24] Christopher T. Hill. Topcolor: Top quark condensation in a gauge extension of the standard model. *Phys.Lett.*, B266:419–424, 1991.
 - [25] Christopher T. Hill and Elizabeth H. Simmons. Strong dynamics and electroweak symmetry breaking. *Phys.Rept.*, 381:235–402, 2003.
 - [26] Bogdan A. Dobrescu and Christopher T. Hill. Electroweak symmetry breaking via top condensation seesaw. *Phys.Rev.Lett.*, 81:2634–2637, 1998.
 - [27] R. Sekhar Chivukula, Bogdan A. Dobrescu, Howard Georgi, and Christopher T. Hill. Top

- quark seesaw theory of electroweak symmetry breaking. *Phys.Rev.*, D59:075003, 1999.
- [28] Hong-Jian He, Timothy M.P. Tait, and C.P. Yuan. New top flavor models with seesaw mechanism. *Phys.Rev.*, D62:011702, 2000.
 - [29] Hidenori S. Fukano and Kimmo Tuominen. A hybrid 4th generation: Technicolor with top-seesaw. 2012.
 - [30] Roberto Contino, Leandro Da Rold, and Alex Pomarol. Light custodians in natural composite Higgs models. *Phys.Rev.*, D75:055014, 2007.
 - [31] Marcela S. Carena, Eduardo Ponton, Jose Santiago, and Carlos E.M. Wagner. Light Kaluza Klein States in Randall-Sundrum Models with Custodial SU(2). *Nucl.Phys.*, B759:202–227, 2006.
 - [32] Riccardo Barbieri, B. Bellazzini, Vyacheslav S. Rychkov, and Alvise Varagnolo. The Higgs boson from an extended symmetry. *Phys.Rev.*, D76:115008, 2007.
 - [33] Oleksii Matsedonskyi, Giuliano Panico, and Andrea Wulzer. Light Top Partners for a Light Composite Higgs. 2012.
 - [34] P. Bamert, C.P. Burgess, James M. Cline, David London, and E. Nardi. R(*b*) and new physics: A Comprehensive analysis. *Phys.Rev.*, D54:4275–4300, 1996.
 - [35] D. Comelli and Joao P. Silva. Decoupling or nondecoupling: Is that the R(*b*) question? *Phys.Rev.*, D54:1176–1181, 1996.
 - [36] Giacomo Cacciapaglia, Aldo Deandrea, Daisuke Harada, and Yasuhiro Okada. Bounds and Decays of New Heavy Vector-like Top Partners. *JHEP*, 1011:159, 2010.
 - [37] K. Nakamura et al. Review of particle physics. *J.Phys.G*, G37:075021, 2010.
 - [38] A.A. Akhundov, D. Yu. Bardin, and T. Riemann. Electroweak One Loop Corrections to the Decay of the Neutral Vector Boson. *Nucl.Phys.*, B276:1, 1986.
 - [39] J. Bernabeu, A. Pich, and A. Santamaria. $\Gamma(Z \rightarrow b\bar{b})$: A Signature of Hard Mass Terms for a Heavy Top. *Phys.Lett.*, B200:569, 1988.
 - [40] Wim Beenakker and Wolfgang Hollik. The Width of the Z Boson. *Z.Phys.*, C40:141, 1988.
 - [41] C.P. Burgess, Stephen Godfrey, Heinz Konig, David London, and Ivan Maksymyk. Model independent global constraints on new physics. *Phys.Rev.*, D49:6115–6147, 1994.
 - [42] Howard E. Haber and Heather E. Logan. Radiative corrections to the Z *b* anti-*b* vertex and constraints on extended Higgs sectors. *Phys.Rev.*, D62:015011, 2000.
 - [43] Precision electroweak measurements on the *Z* resonance. *Phys.Rept.*, 427:257–454, 2006. 302

- pages, v2: minor corrections and updates of references. Accepted for publication by Physics Reports, v3: further small corrections and journal version Report-no: CERN-PH-EP/2005-041, SLAC-R-774.
- [44] Michael E. Peskin and Tatsu Takeuchi. Estimation of oblique electroweak corrections. *Phys.Rev.*, D46:381–409, 1992.
 - [45] Guido Altarelli and Riccardo Barbieri. Vacuum polarization effects of new physics on electroweak processes. *Phys. Lett.*, B253:161–167, 1991.
 - [46] Riccardo Barbieri, Alex Pomarol, Riccardo Rattazzi, and Alessandro Strumia. Electroweak symmetry breaking after LEP-1 and LEP-2. *Nucl.Phys.*, B703:127–146, 2004.
 - [47] M. Baak et al. Updated Status of the Global Electroweak Fit and Constraints on New Physics. 2011.
 - [48] W. Hollik. Electroweak radiative corrections. 1993.
 - [49] Mu-Chun Chen, Sally Dawson, and C.B. Jackson. Higgs Triplets, Decoupling, and Precision Measurements. *Phys.Rev.*, D78:093001, 2008.
 - [50] Georges Aad et al. Search for pair production of a heavy quark decaying to a W boson and a b quark in the lepton+jets channel with the ATLAS detector. 2012.
 - [51] Georges Aad et al. Search for pair production of a new quark that decays to a Z boson and a bottom quark with the ATLAS detector. *Phys.Rev.Lett.*, 2012. Long author list - awaiting processing.
 - [52] Serguei Chatrchyan et al. Search for heavy, top-like quark pair production in the dilepton final state in pp collisions at $\sqrt{s} = 7$ TeV. 2012. Submitted to Physics Letters B.
 - [53] Serguei Chatrchyan et al. Search for heavy bottom-like quarks in 4.9 inverse femtobarns of pp collisions at $\sqrt{s} = 7$ TeV. 2012.
 - [54] Serguei Chatrchyan et al. Search for a Vector-like Quark with Charge 2/3 in $t + Z$ Events from pp Collisions at $\sqrt{s} = 7$ TeV. *Phys.Rev.Lett.*, 107:271802, 2011.
 - [55] J.A. Aguilar-Saavedra. Identifying top partners at LHC. *JHEP*, 0911:030, 2009.
 - [56] Christian J. Flacco, Daniel Whiteson, and Matthew Kelly. Fourth generation quark mass limits in CKM-element space. 2011.
 - [57] Giacomo Cacciapaglia, Aldo Deandrea, Luca Panizzi, Naveen Gaur, Daisuke Harada, et al. Heavy Vector-like Top Partners at the LHC and flavour constraints. *JHEP*, 1203:070, 2012.
 - [58] Keisuke Harigaya, Shigeki Matsumoto, Mihoko M. Nojiri, and Kohsaku Tobioka. Search for

- the Top Partner at the LHC using Multi-b-Jet Channels. 2012.
- [59] Joshua Berger, Jay Hubisz, and Maxim Perelstein. A Fermionic Top Partner: Naturalness and the LHC. 2012.
 - [60] J.A. Aguilar-Saavedra. Effects of mixing with quark singlets. *Phys.Rev.*, D67:035003, 2003.
 - [61] Monika Blanke, Andrzej J. Buras, Anton Poschenrieder, Cecilia Tarantino, Selma Uhlig, et al. Particle-Antiparticle Mixing, ε_K , $\Delta\Gamma_q$, A_{SL}^q , $A_{\text{CP}}(B_d \rightarrow \psi K_S)$, $A_{\text{CP}}(B_s \rightarrow \psi\phi)$ and $B \rightarrow X_{s,d}\gamma$ in the Littlest Higgs Model with T-Parity. *JHEP*, 0612:003, 2006.
 - [62] L. Lavoura and Joao P. Silva. Bounds on the mixing of the down type quarks with vector - like singlet quarks. *Phys.Rev.*, D47:1117–1126, 1993.
 - [63] Marko B. Popovic and Elizabeth H. Simmons. Weak singlet fermions: Models and constraints. *Phys.Rev.*, D62:035002, 2000.
 - [64] Tevatron Electroweak Working Group. Combination of CDF and D0 Results on the Mass of the Top Quark. 2009. FERMILAB-TM-2427-E, TEVEWWG/top 2009/03, CDF Note 9717, D0-NOTE-5899 15 pages, 1 figure.
 - [65] Michael S. Chanowitz, M. A. Furman, and I. Hinchliffe. Weak Interactions of Ultraheavy Fermions. 2. *Nucl. Phys.*, B153:402, 1979.
 - [66] S. Dawson and P. Jaiswal. Four Generations, Higgs Physics, and the MSSM. *Phys.Rev.*, D82:073017, 2010.
 - [67] Fred Jegerlehner. Renormalizing the standard model. *Conf.Proc.*, C900603:476–590, 1990.
 - [68] G. Cynolter and E. Lendvai. Electroweak Precision Constraints on Vector-like Fermions. *Eur.Phys.J.*, C58:463–469, 2008.
 - [69] Nobuhiro Maekawa. Electroweak symmetry breaking by vector - like fermions’ condensation with small S and T parameters. *Phys.Rev.*, D52:1684–1692, 1995.
 - [70] Hong-Jian He, Christopher T. Hill, and Timothy M.P. Tait. Top quark seesaw, vacuum structure and electroweak precision constraints. *Phys.Rev.*, D65:055006, 2002.
 - [71] Csaba Csaki, Jay Hubisz, Graham D. Kribs, Patrick Meade, and John Terning. Variations of little Higgs models and their electroweak constraints. *Phys.Rev.*, D68:035009, 2003.
 - [72] Yang Bai, JiJi Fan, and JoAnne L. Hewett. Hiding a Heavy Higgs Boson at the 7 TeV LHC. 2011.
 - [73] P. Bamert. $R(b)$ and heavy quark mixing. 1996.
 - [74] Charalampos Anastasiou, Elisabetta Furlan, and Jose Santiago. Realistic Composite Higgs

- Models. *Phys.Rev.*, D79:075003, 2009.
- [75] Marcela S. Carena, Eduardo Ponton, Jose Santiago, and C.E.M. Wagner. Electroweak constraints on warped models with custodial symmetry. *Phys.Rev.*, D76:035006, 2007.
 - [76] L. Lavoura and Joao P. Silva. The Oblique corrections from vector - like singlet and doublet quarks. *Phys.Rev.*, D47:2046–2057, 1993.
 - [77] Frank Wilczek. Decays of Heavy Vector Mesons Into Higgs Particles. *Phys.Rev.Lett.*, 39:1304, 1977.
 - [78] John R. Ellis, M.K. Gaillard, Dimitri V. Nanopoulos, and Christopher T. Sachrajda. Is the Mass of the Higgs Boson About 10-GeV? *Phys.Lett.*, B83:339, 1979.
 - [79] H.M. Georgi, S.L. Glashow, M.E. Machacek, and Dimitri V. Nanopoulos. Higgs Bosons from Two Gluon Annihilation in Proton Proton Collisions. *Phys.Rev.Lett.*, 40:692, 1978.
 - [80] Adam Falkowski. Pseudo-goldstone Higgs production via gluon fusion. *Phys.Rev.*, D77:055018, 2008.
 - [81] Ian Low, Riccardo Rattazzi, and Alessandro Vichi. Theoretical Constraints on the Higgs Effective Couplings. *JHEP*, 1004:126, 2010.
 - [82] Bogdan A. Dobrescu, Graham D. Kribs, and Adam Martin. Higgs Underproduction at the LHC. *Phys.Rev.*, D85:074031, 2012. 8 pages, 9 figures. Minor improvements made and references added.
 - [83] Christoph Englert, Tilman Plehn, Michael Rauch, Dirk Zerwas, and Peter M. Zerwas. LHC: Standard Higgs and Hidden Higgs. *Phys.Lett.*, B707:512–516, 2012. 7 pages, 3 figures/ references added/ final version accepted for publication in PLB.
 - [84] J.R. Espinosa, C. Grojean, and M. Muhlleitner. Composite Higgs under LHC Experimental Scrutiny. 2012. 6 pages. Contribution to the proceedings of Hadron Collider Physics Symposium 2011, Paris Nov. 14-18.
 - [85] Dean Carmi, Adam Falkowski, Eric Kuflik, and Tomer Volansky. Interpreting LHC Higgs Results from Natural New Physics Perspective. 2012.
 - [86] Aleksandr Azatov, Roberto Contino, and Jamison Galloway. Model-Independent Bounds on a Light Higgs. *JHEP*, 1204:127, 2012.
 - [87] J.R. Espinosa, Christophe Grojean, M. Muhlleitner, and Michael Trott. Fingerprinting Higgs Suspects at the LHC. 2012.
 - [88] Pier Paolo Giardino, Kristjan Kannike, Martti Raidal, and Alessandro Strumia. Reconstruct-

- ing Higgs boson properties from the LHC and Tevatron data. 2012. 15 pages, 5 figures, references added, discussion clarified (e.g. fit to invisible width), fit to radion added.
- [89] John Ellis and Tevong You. Global Analysis of Experimental Constraints on a Possible Higgs-Like Particle with Mass ~ 125 GeV. 2012.
- [90] Markus Klute, Remi Lafaye, Tilman Plehn, Michael Rauch, and Dirk Zerwas. Measuring Higgs Couplings from LHC Data. 2012.